INTRODUCTION

INJURY TO THE CENTRAL NERVOUS SYSTEM (CNS) causes permanent defects in neurologic function. A number of animal experiments involving neural cell transplantation after neural damage, including spinal cord injury (SCI), have been conducted to investigate the replacement of injured neural components and functional recovery after injury to the CNS. Beneficial effects have been reported with Schwann cells (Martin et al., 1996), olfactory ensheathing cells (Doucette, 1995), embryonic stem cells (McDonald et al., 1999), neural stem cells (Ogawa et al., 2002), and choroid plexus ependymal cells (Ide et al., 2001) for such transplantation. However, the transplantation of expanded and/or allogenic cells in human patients requires addressing such issues as immunologic reactivity to such transplantation and the therapeutic time window during which it is effective. Furthermore, clinical trials of neural cell transplantation after stroke have revealed that simple cell transplantation has only a mild therapeutic effect (Kondziolka et al., 2000), probably because of the absence of a favorable environment for reconstitution of the neural system (Taguchi et al., 2004).

Recently, a highly neovascularized environment after injury to the CNS, obtained by hematopoietic stem cell transplantation, was shown to accelerate recovery of neurologic function in a model of stroke (Taguchi et al., 2004). Additionally, clinical trials found that transplantation of bone marrow–derived mononuclear cells (BM-MNC) had beneficial effects on functional recovery after myocardial infarction (Assmus et al., 2002; Strauer et al., 2002). BM-MNC are known to include immature cells such as hematopoietic stem cells and endothelial progenitor cells, and have also been shown to supply multiple growth factors (Rehman et al., 2003) that may protect against secondary neural injury (Widenfalk et al., 2003). We therefore investigated the effect of transplanting BM-MNC in a rat model of SCI, and found that it had a neuroprotective effect that promoted functional improvement.

METHODS

All procedures were performed in accordance with the Guidelines for Animal Experiments of Kyoto University. Quantitative measurements and behavioral tests were performed by investigators unaware of the experimental protocol and the identity of the sections/animals under study.

Preparation of Bone Marrow–Derived Mononuclear Cells

Bone marrow cells were obtained from 8-week-old (adult) male Wistar rats weighing 200–220 g. Cells were harvested after administration of 5–fluorouracil, as described previously (Azizi et al., 1998). BM-MNC were separated by density centrifugation with a commercially available density solution (density, 1.077; Lymphoprep™; Nycomed Pharma, Oslo, Norway; www.nycomed.com) (Tomita et al., 2002). These cells were assessed on the basis of cell surface markers (PharMingen, San Diego, CA), using a fluorescence-activated cell sorter, and the following percentages were found to express the respective markers, which are markers of Thy-1, leukocytes, β1-integrin, c-kit, hematopoietic stem cells, endothelial cells, and macrophages, respectively: 43% CD90, 38% CD45, 74% CD29, 11% CD117, 10% CD34, 24% CD31, and 19% CD11b/c.

To trace cells, BM-MNC were labeled with the fluorescent membrane-intercalating dye PKH67 (green fluorescence; MINI-67; Sigma, St. Louis, MO) (Tomita et al., 2002).

Spinal Cord Injury and Transplantation of BM-MNC

Crush injury was produced in the spinal cords of 40 Wistar rats, all 4 weeks old, by impact with a weight-drop device (NYU Spinal Cord Contusion System; New York University, New York, NY) as previously described (Bai et al., 2003). The rats were anesthetized with pentobarbital 50 mg/kg i.p., laminectomy was done at the level of Th8–9, and injury was achieved by dropping a 10-g weight 2.5 mm in diameter from a height of 12.5 mm (Bai et al., 2003). At 1 h after injury, a cell suspension of 5×10^6 viable BM-MNC, dissolved in 70 μL of Hanks' balanced salt solution (HBSS), was injected with an insulin syringe and stereotaxic coordinates into the fourth ventricles of 20 Wistar rats over a period of 5 min, as previously described (Bai et al., 2003). A control population of 20 rats underwent the same crush injury procedure followed by injection of the same volume of HBSS but without the cell suspension. A total of 18 rats with SCI (n = 9 per group) were used for histologic examination and evaluation in the acute stage of injury. Three rats per group were killed, on days 1, 3, and 7, respectively. A total of six rats with SCI (n = 3 per group) were killed on day 3 for the measurement of cytokines in CSF by enzyme-linked immunosorbent assay (ELISA). Sixteen rats with SCI (n = 8 per group) were tested according to the Basso–Beattie–Bresnahan (BBB) locomotor rating scale (Basso et al., 1995), to evaluate

locomotor function of the hindlimbs before injury and again on days 1, 7, 14, 21, 28, and 35. On day 35, these rats were killed for histologic study.

Preparation of Tissues for Histologic Analysis

A fixative containing 4% paraformaldehyde in 0.1 M phosphate buffer was perfused through the hearts of all rats. Sections of spinal cord tissue 10–μm-thick were subsequently cut longitudinally with a cryostat and mounted on glass slides for observation after staining with hematoxylin and eosin (H&E) or immunohistochemical staining. The following primary antibodies and dilutions were used: mouse monoclonal antibody (Mab) against glial fibrillary acidic protein (GFAP; Sigma) at 1:400; mouse Mab against β-tubulin type III (Sigma) at 1:300; and rabbit polyclonal antibody against von Willebrand Factor (vWF; DAKO, Glostrup, Denmark) at 1:10. A fragment-conjugated goat antimouse antibody (Alexa Fluor; Molecular Probes, Eugene, OR) at a dilution of 1:1000, and a fragment-conjugated goat antirabbit antibody (Alexa Fluor; Molecular Probes) at a dilution of 1:500, were used as second antibodies. To stain for cell nuclei, we used the membrane-impermeant fluorescent DNA-binding dye TO-PRO-3 (Invitrogen, Carlsbad, CA) at a dilution of 1:500.

Evaluation of Apoptotic Cells at the Site of SCI in the Acute Stage of Injury

To quantitate apoptotic cells at the site of injury on day 3 after SCI (n = 3 per group), we used a terminal deoxynucleotidyl transferase-mediated deoxyuridine triphosphate (dUTP)–biotin nick-end labeling (TUNEL) assay (DeadEnd™ Fluorometric TUNEL System; Promega) according to the protocol recommended by the manufacturer. We examined five parasagittal sections of injured spinal cord, including the median sagittal section, and compared the numbers of TUNEL-positive cells per field (0.1 mm^2) at high magnification (×40) among the different groups of animals.

Quantification of Protected Axons in the Acute Stage of Injury

To investigate the degree of protection of nerve fibers provided by BM-MNC transplantation in the acute stage of SCI, we used immunohistochemical staining of sections obtained at the injury site, with an anti-β-tubulin type III antibody. We did this on six rats on day 3 after SCI (n = 3 per group) and a further six animals on day 7 (n = 3 per group). We examined a total of 21 sagittal sections obtained from each animal, consisting of one median sagittal section and two sets of 10 consecutive sections cut at intervals of 50 μm from the median plane laterally toward the left (one set) and right (the other set). These sections covered two-thirds of the width of the spinal cord, including whole degenerated nerve fibers. We measured the density of nerve fibers that stained positively for β-tubulin type III at the site of injury within 2.5 mm in the cephalocaudal direction, using the image processing and analysis software NIH Image 1.61. The density of nerve fibers was reported as the percentage of the β-tubulin type III-positive area relative to the entire area of SCI.

Blood Vessels at the Site of Injury in the Acute Stage of Injury

Blood vessels were examined at the site of injury on days 3 and 7. Five parasagittal sections, including the median sagittal section, obtained from the injury site in each animal, were stained for vWF and TO-PRO-3. vWF-positive cells were observed mainly around the center of the injury site. Using NIH Image 1.61 software, we measured the density of vWF-positive cells in sagittal sections centered around and within 2.5 mm of the injury site in the cephalocaudal direction.

ELISA of Cytokines in Cerebrospinal Fluid

We sought to determine whether transplantation of BM-MNC after SCI had an effect on neuroprotective or angiogenic factors in CSF. CSF was obtained from six rats (n = 3 per group) on day 3 after SCI and assayed via ELISA for vascular endothelial growth factor (VEGF) (Immuno-Biological Laboratories, Gunma, Japan), hepatocyte growth factor (HGF) (Institute of Immunology, Tokyo, Japan), and tumor necrosis factor-α (TNF-α) (BioSource International, Camarillo, CA), following the manufacturers' recommended protocols in each assay.

Measurement of Injury-Cavity Volume

The volume of each cavity that developed after SCI was quantified as described previously (Ohta et al., 2004) at 35 days after injury (n = 8 per group). Briefly, horizontal cryostat sections were stained with H&E and examined under a light microscope equipped with a charge-coupled-device (CCD) camera (HC300; Fuji Photo Film Co. Ltd., Tokyo, Japan) (Reyes and Verfaillie, 2001). We used a total of 41 sagittal sections obtained from each animal, consisting of one median sagittal section and two sets of 20 consecutive sections cut at intervals of 50 μm from the median plane laterally toward the left (one set) and right (the other set). These sections covered the entire spinal cord. The area of cavitation in each spinal cord section was measured, as shown in Figure 6G below, using NIH Image 1.61 software. The cavity volume was then calculated by multiplying the average area of cavi-

tation by the depth of the section examined (Takami et al., 2002).

Quantification of Angiogenesis Around the Injury Cavity

We counted the blood vessels around the injury cavity in each rat at 35 days after injury. Vessel density was defined as the number of blood vessels per injury area immediately around the cavity. We investigated the number of blood vessels that stained immunopositively for vWF in the marginal zone extending to within 200 μm of the inner margin of the injury cavity (see Fig. 6I,K below).

Behavioral Analysis

The animals' locomotor activity was evaluated by means of open-field BBB scoring, as described previously (Basso et al., 1995; Wu et al., 2003). Briefly, the behavior of each animal in an open 75 × 120-cm field was observed by two researchers. Scores ranging from 0 (complete paralysis) to 21 (normal gait) were recorded every week after surgery.

Statistical Analysis

Differences in cavity formation and the density of vWF-positive cells on day 35 were analyzed by unpaired Student's *t*-tests. Differences in the concentration of cytokines in CSF, the density of nerve fibers and vWF-positive cells in the acute stage of injury, and BBB score were analyzed with the Mann-Whitney *U*-test. A value of $p < 0.05$ was considered statistically significant.

RESULTS

Functional Recovery after Spinal Cord Injury

BBB locomotor scores are shown in Figure 1. The maximum BBB score was 21 before SCI, while the initial BBB score for the spinal cord–injured rats was less than 8. No significant functional improvement was observed at 24 h after SCI in rats that underwent cell transplantation as compared to control rats. However, continuous functional recovery was observed at days 7–35 in rats that underwent BM-MNC transplantation. In contrast, little, if any, functional recovery was observed in control rats. The functional recovery seen in the rats that underwent BM-MNC transplantation was significant.

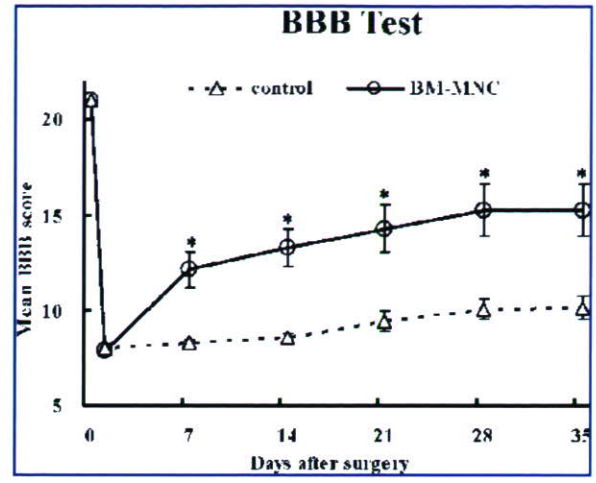

FIG. 1. Administration of BM-MNC promotes rapid improvement of motor function after SCI. To evaluate motor function of the lower limbs, BBB locomotor scores were determined on days 1, 7, 14, 21, 28, and 35 after SCI. Scores range from 0 (complete paralysis) to 21 (normal gait). On day 1 there was no significant difference in the mean score between BM-MNC-transplanted and control groups of animals. However, from day 7 to day 35, the mean scores of rats that underwent BM-MNC transplantation were significantly higher than those of control rats ($n = 8$ per group). *$p < 0.05$ versus control.

Transplanted BM-MNC in the Fourth Ventricle and around the Injured Spinal Cord

To trace transplanted BM-MNC labeled with PKH67 (green fluorescence), we examined the fourth ventricle of the rat brain and the injured spinal cord. At 1 day after transplantation, PKH67-labeled cells were observed very close to the choroid plexus in the ventricle (Fig. 2A,B), as well as on the surface of the pia mater of the injured spinal cord (Fig. 2C–E). On day 3, these cells decreased in number, and a piece of transplanted cell was sometimes seen in the ventricle (Fig. 2F), while some transplanted cells were integrated into the pia mater of the injured cord (Fig. 2G–I). On day 7, few, if any, PKH67–labeled cells were observed in the ventricle (Fig. 2J) or around the injured spinal cord (Fig. 2K–M).

Protection of Axons at the Site of Injury in the Acute Stage

To investigate whether BM-MNC have a protective effect on nerve fibers within 1 week after SCI, we performed immunohistochemistry for β-tubulin type III on sections of injured spinal cord on day 3 (Fig. 3A,B) and day 7 (Fig. 3C,D) after injury. In control rats (Fig. 3A,C), the area not stained had often spread to the dorsal side of the spinal cord, where direct contusion injury had occurred. In contrast, in BM-MNC-transplanted rats (Fig. 3B,D), the unstained area was restricted and was smaller than in control rats.

To investigate whether transplantation of BM-MNC protects injured spinal cord from apoptosis, we performed

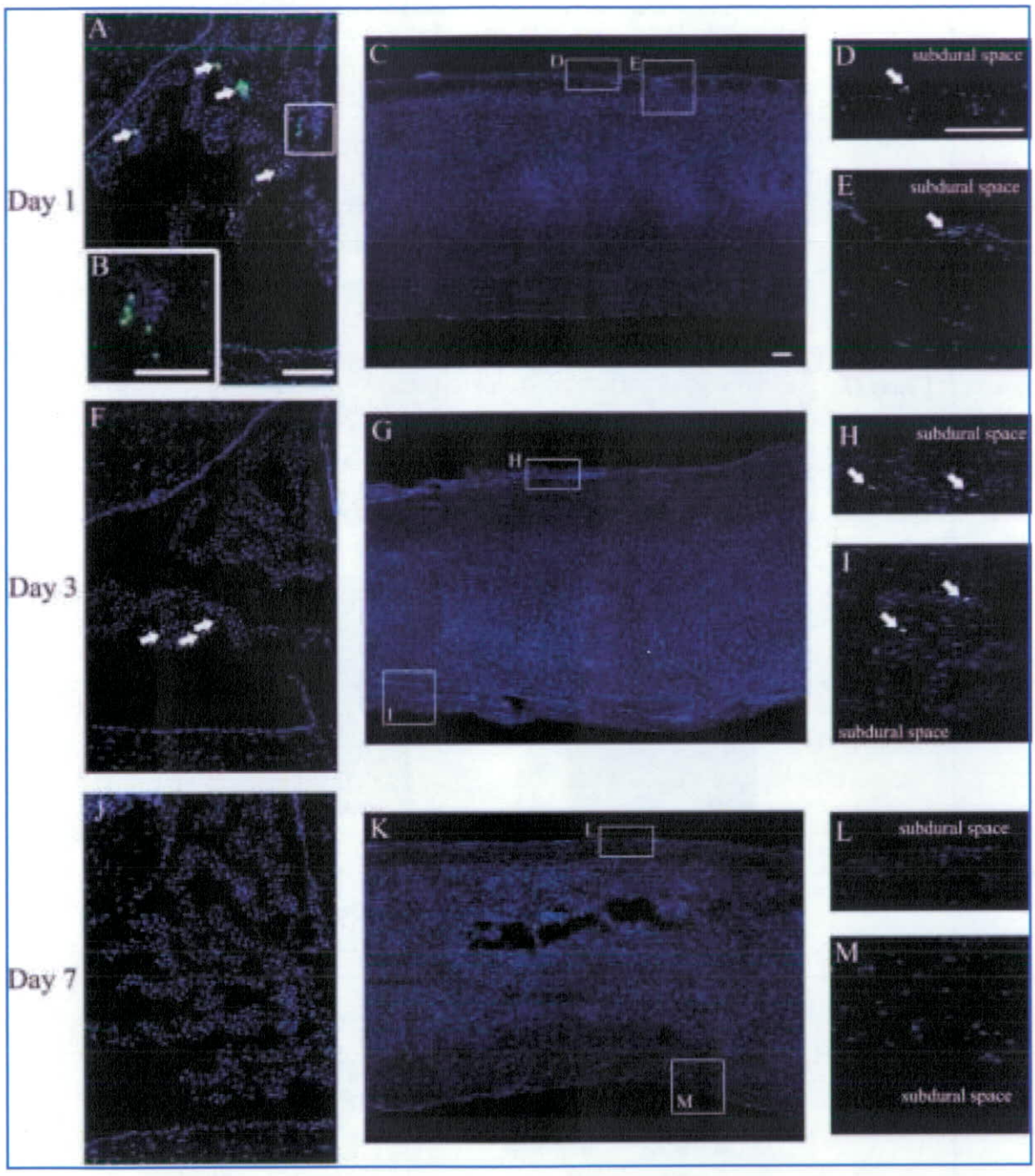

FIG. 2. Transplanted BM-MNC (arrows) were observed in the fourth ventricle and around the site of spinal cord injury (sagittal section). (**A–E**) On day 1 after transplantation, BM-MNC, labeled with PKH67 (green fluorescence), were observed very close to the choroid plexus in the ventricle (B is a magnified view of the box in A). Some transplanted cells became attached to the surface of the pia mater of the injured spinal cord (D and E are magnified views of the boxes in C). (**F–I**) On day 3, a few transplanted cells were seen in the ventricle (F), and some transplanted cells were integrated into the pia mater of the injured cord (H and I are magnified views of the boxes in G). (**J–M**) On day 7, almost no PKH67-labeled cells were observed (L and M are magnified views of the boxes in K). Nuclei were stained with TO-PRO-3 (blue). Scale bar = 100 μm (A–D).

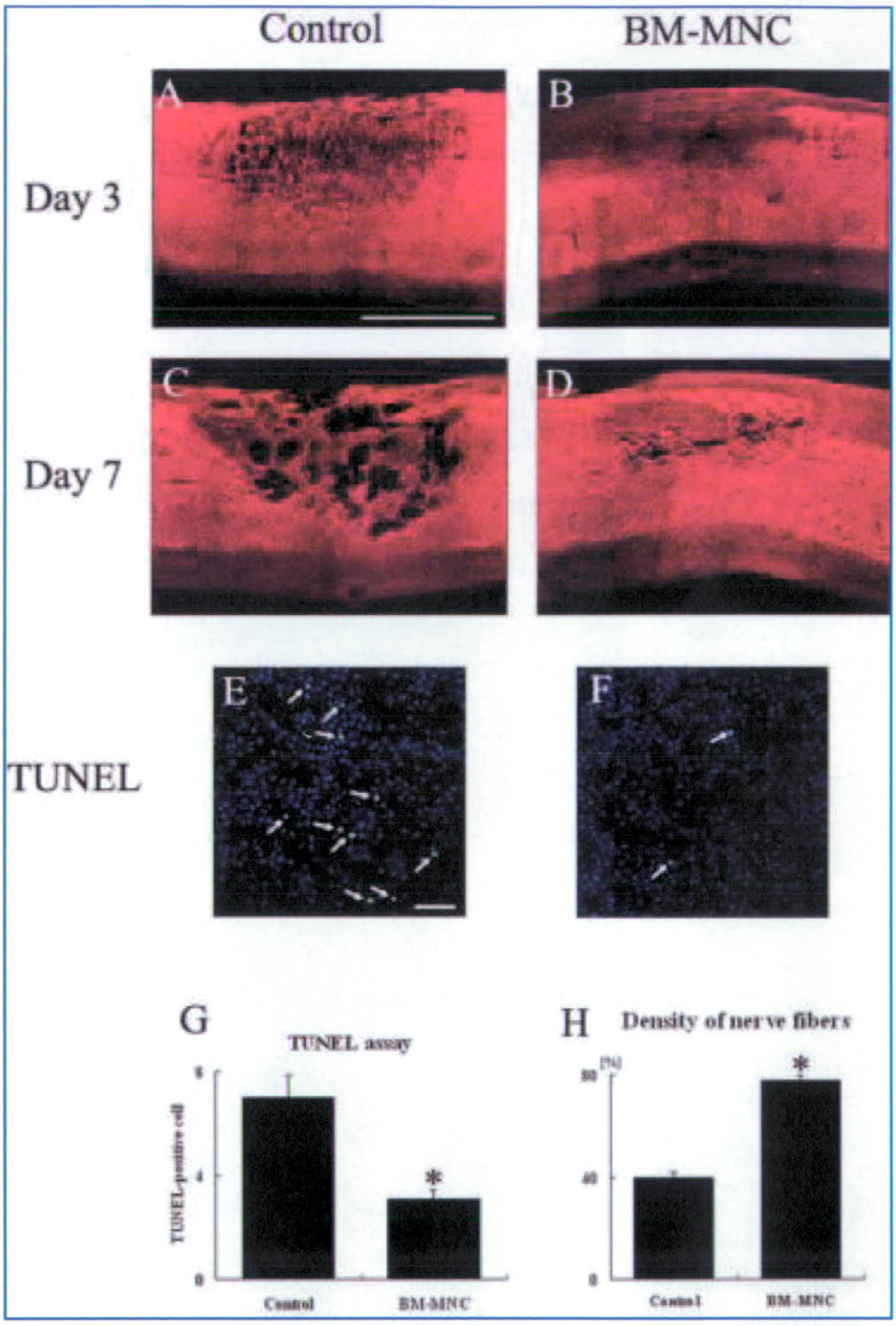

FIG. 3. Administration of BM-MNC reduced the number of apoptotic cells at the site of injury in the acute stage. (**A–D**) Sagittal sections obtained from the injury site on day 3 (A,B) and day 7 (C,D) were stained for β-tubulin type III. Axons stained for β-tubulin type III were preserved at the site of injury in BM-MNC-transplanted (B,D) compared to control rats (A,C). (**E,F**) TUNEL of fragmented DNA was performed on sagittal sections obtained on day 3 from the injury sites of control rats (E) and BM-MNC-transplanted rats (F). TUNEL-positive nuclei (green) were merged with cell nuclei (blue) as indicated by arrows. (**G**) The number of TUNEL-positive cells was significantly smaller in BM-MNC-transplanted than in control rats ($n = 3$ per group). $^*p < 0.01$ versus control. (**H**) The density of nerve fibers at the site of injury on day 7 was significantly higher in BM-MNC-transplanted than in control rats ($n = 3$ per group). $^*p < 0.05$ versus control. Scale bar = 1 mm (A), 50 μm (E).

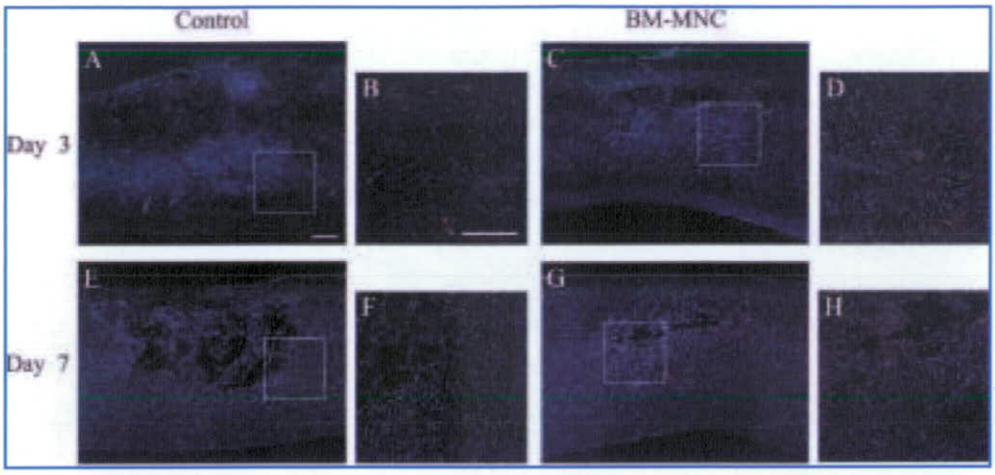

FIG. 4. Blood vessels stained for vWF at the site of SCI in the acute stage of injury. Immunohistochemical analysis of vWF (red) was performed on sagittal sections at the site of injury on day 3 (**A–D**) and day 7 (**E–H**) in animals treated with HBSS (A,B,E,F) or BM-MNC (C,D,G,H). Nuclei were stained with TO-PRO-3 (blue). vWF-positive cells were identified mainly around the center of the injured spinal cord (A–H). The figures in the right column (B,D,F,H) are magnified views of the boxes in A, C, E, and G, respectively. Scale bar = 200 μm (A,B).

TUNEL assays on sections obtained from the injury site on day 3 (Fig. 3E,F) after injury. TUNEL-positive (green) cells were observed mainly around the tissue not stained for β-tubulin type III at the injury site. The number of TUNEL-positive cells per high-power field (hpf) was significantly lower in BM-MNC-transplanted rats than in control rats (Fig. 3G). Consistent with these findings was a significantly higher density of nerve fibers stained for β-tubulin type III in BM-MNC-transplanted rats than in control rats (Fig. 3H).

To evaluate distribution of blood vessels at the site of injury, we performed immunohistochemistry for vWF on sections obtained on day 3 (Fig. 4A–D) and day 7 (Fig. 4E–H) after SCI. vWF-positive cells (red) were distributed mainly around the center of the injured spinal cord. Quantitative analysis revealed no significant difference between BM-MNC-transplanted rats and control rats in the density of vWF-positive cells at the injury site on day 7 (9.84 ± 0.83 vs. 10.8 ± 1.64 cells/mm^2, respectively; $p = 0.34$).

Increase in Hepatocyte Growth Factor Concentration in CSF with BM-MNC Transplantation

On day 3 after SCI, we obtained CSF and measured the concentrations in it of VEGF, HGF, and TNF-α by ELISA. The concentration of VEGF, a well-known an-

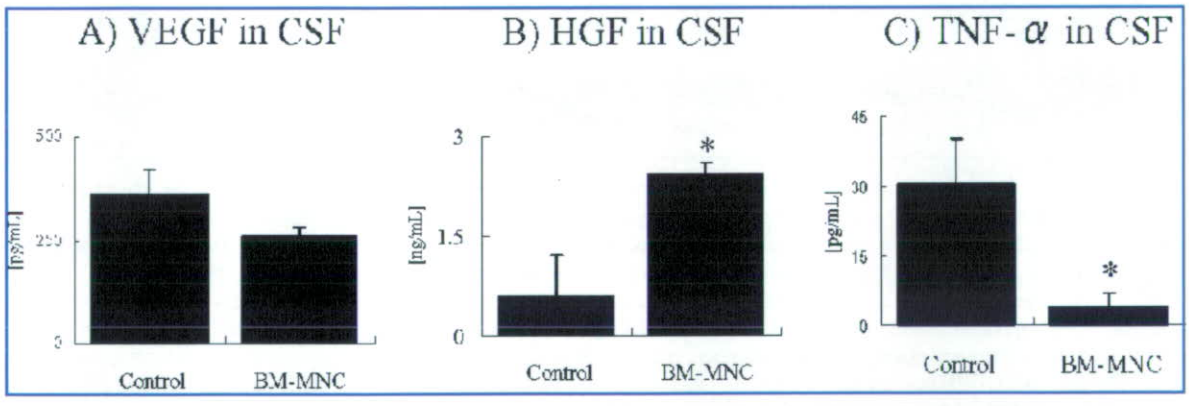

FIG. 5. Determination of concentrations of cytokines in CSF by ELISA. CSF was obtained from rats on day 3 after SCI. No significant difference was found in the concentration of VEGF in BM-MNC-transplanted and control animals (**A**). However, the concentration of HGF was remarkably higher in CSF from BM-MNC-transplanted rats than in that of control rats (**B**). A lower concentration of TNF-α was observed in the CSF of BM-MNC-transplanted than in that of control rats (**C**) ($n = 3$ per group). *$p < 0.05$ versus control.

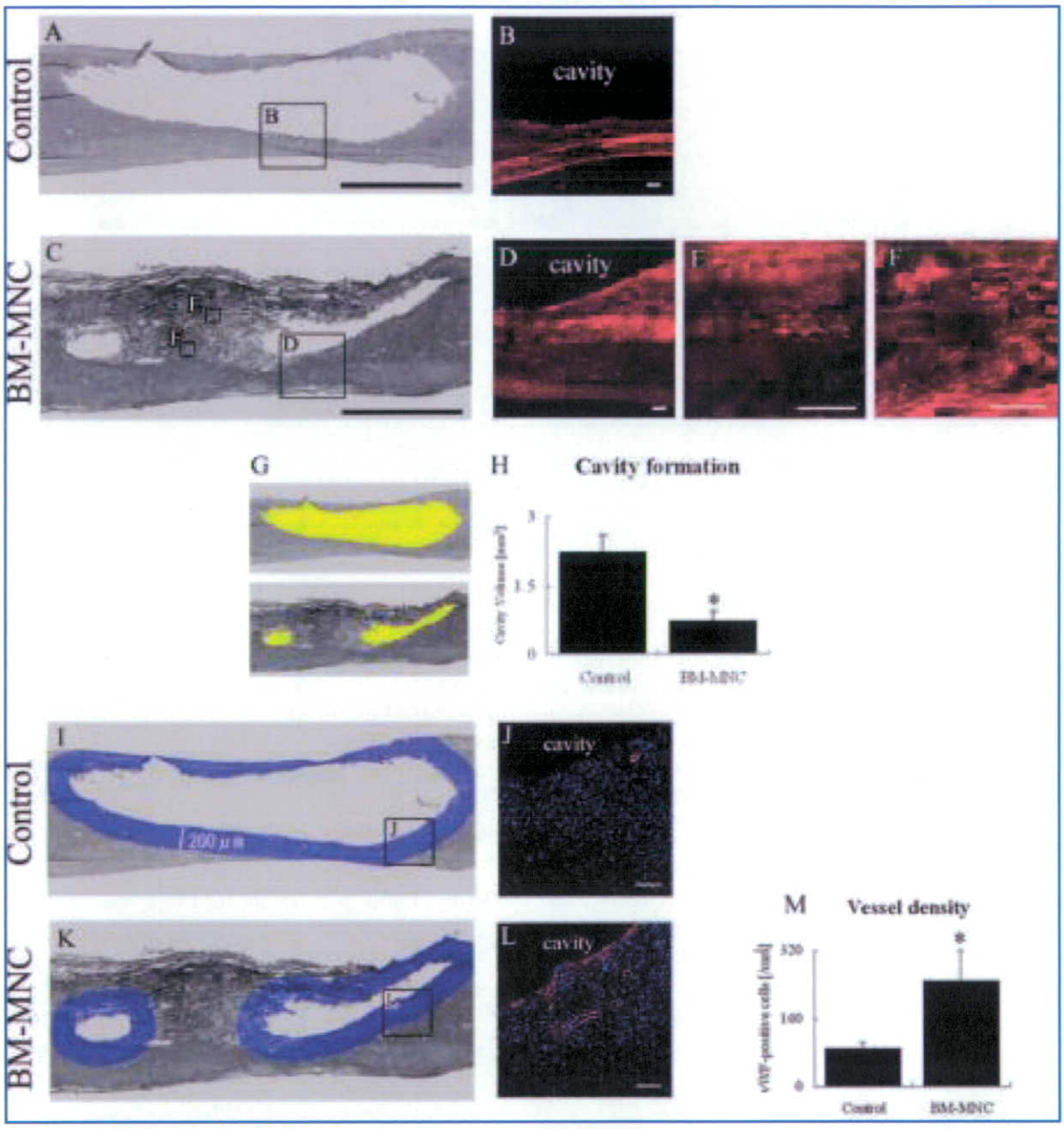

FIG. 6. Injured spinal cord on day 35 after SCI. (**A–H**) Although clear cavity formation was observed at the site of injury in control rats (A, H&E staining; B, staining for β-tubulin type III), only limited cavity formation was observed in BM-MNC-transplanted rats (C, H&E staining; D, staining for β-tubulin type III). Expression of β-tubulin type III (E) and GFAP (F) was confirmed in the tissue around the cavity. The area of the cavity was measured as indicated by yellow in G (H&E staining) in consecutive sagittal sections, and the volume of the cavity was calculated. A significant reduction in the cavity volume was found in BM-MNC-transplanted rats as compared to control rats (H; $n = 8$ per group). *$p = 0.01$ versus control. (**I–M**) Blood vessels stained for vWF (red) were observed in the marginal zone of the cavities of control rats (I,J) and BM-MNC-transplanted rats (K,L). The density of vWF-positive cells in the marginal zone, indicated by blue (I,K), was significantly increased in BM-MNC-transplanted as compared to control rats (M; $n = 8$). *$p < 0.05$ versus control. Scale bar = 1 mm (A,C), 100 μm (B,D–F,J,L).

giogenic factor (Carmeliet, 2003), did not show a significant increase with BM-MNC transplantation (Fig. 5A). This result was consistent with our finding that, in the acute stage of injury, there was no increase in the number of cells stained for vWF as a vascular marker. In contrast, we observed a remarkable increase in the concentration of HGF, which is known to have neuroprotective effects *in vivo* and *in vitro* (Tsuzuki et al., 2000; Zhang et al., 2000), with BM-MNC transplantation (Fig. 5B). These results may explain the decrease in concentration of TNF-α with BM-MNC transplantation (Fig. 5C).

Prevention of Cavity Formation in the Chronic Stage

To investigate whether BM-MNC have an inhibitory effect on degeneration of the injured spinal cord in the chronic stage of injury, we conducted a histologic study on sections obtained from the injury site on day 35 after SCI. SCI is known to cause secondary injury accompanied by inflammation, followed by cavity formation (Zhang and Guth, 1997). On day 35, clear cavity formation was observed in control rats (Fig. 6A, H&E staining; Fig. 6B, staining for β-tubulin type III). The cavity wall was composed of loosely packed tissue surrounded by numerous empty spaces, with cell nuclei sparsely dispersed throughout the wall. In contrast, limited cavity formation was observed with administration of BM-MNC (Fig. 6C, H&E staining; Fig. 6D, staining for β-tubulin type III). The wall of the cavity, composed of well-packed tissue as in the normal spinal cord, contained many cell nuclei. Tissue around the cavity was stained for β-tubulin type III (Fig. 6E) and GFAP (Fig. 6F). We determined the volume of the cavity at the site of injury by measuring the cavity area in sagittal cross sections (Fig. 6G). The volume of the cavity was significantly reduced in the BM-MNC-transplanted rats as compared with that in the control group (Fig. 6H). Moreover, many cells in the area immediately around the cavity stained for vWF (red), a marker of blood vessels (Fig. 6I–L). In the chronic stage of injury, the density of vWF-positive cells just around the cavity was significantly greater in BM-MNC-transplanted rats (Fig. 6K,L) than in control rats (Fig. 6I,J), as shown in Figure 6M.

DISCUSSION

We found that transplantation of BM-MNC soon after SCI had a neuroprotective effect in the acute stage of injury, promoting functional improvement, which was followed by the suppression of cavity formation.

In the acute stage of SCI, transplantation of BM-MNC protected nerve fibers of the injured spinal cord. Although the exact mechanism by which transplantation of BM-MNC exerts a therapeutic effect is unclear, our results indicate little contribution from VEGF; transplantation of BM-MNC did not significantly increase the VEGF concentration in CSF or promote angiogenesis at the site of injury in the acute stage. In contrast, a remarkable increase in the concentration of HGF in CSF was observed with BM-MNC transplantation. HGF is reported to be secreted by BM-MNC (Liu et al., 2004) and to have a strong antiapoptotic effect in neural injury (Tsuzuki et al., 2000; Zhang et al., 2000). These observations, in addition to the secretion by BM-MNC of other neuroprotective cytokines (Kamihata et al., 2001; Chen et al., 2002; Valable et al., 2003), at least partly explain the beneficial effects observed with BM-MNC transplantation. These neuroprotective effects may also explain the decrease in TNF-α concentration in CSF with transplantation of BM-MNC.

Cavity formation is a characteristic of progressive tissue necrosis, which follows the initial primary cell destruction in injury to the CNS (Zhang and Guth, 1997). Regulating injury in the acute stage has been reported to be the critical factor for controlling the progression of secondary injury to the CNS in SCI (Fitch et al., 1999), and in our study the neuroprotective effect of BM-MNC in the acute stage of injury contributed mainly to suppressing cavity formation in the chronic stage of SCI. In accord with these findings was the observed preservation of blood vessels in the chronic stage of injury with transplantation of BM-MNC. As previously reported, blood vessel formation is essential for the repair of tissue after CNS injury such as SCI (Imperato-Kalmar et al., 1997), brain trauma (Giulian et al., 1989), and brain infarction (Taguchi et al., 2004).

In the present study, no transplanted cells were observed in the injured spinal cord on day 7 after BM-MNC transplantation, indicating that the differentiation of transplanted cells into neural cells made little contribution to the positive effect of transplantation, at least with our protocol. Koshizuka et al. reported that immature hematopoietic stem cells from bone marrow, transplanted in the subacute stage of SCI (at 7 days after injury), differentiate into neural precursor cells, which may result in functional recovery partly through neurogenesis (Koshizuka et al., 2004). It has been shown that stem cell transplantation can improve neurologic function by several mechanisms, some of which are neuroprotective effects on host neurons from trophic factors secreted by transplanted cells, and/or the reestablishment of functional neural networks through the integration of transplanted cells (Lindvall and Kokaia, 2004). These observations suggest at least two critical mechanisms by which BM-MNC transplantation may promote functional re-

covery: neuroprotection, when the BM-MNC are transplanted in the hyperacute stage, and differentiation into neural cells, when BM-MNC are transplanted in the subacute stage.

Besides being studied in animal models of various diseases (Kamihata et al., 2001; Shintani et al., 2001), transplantation of BM-MNC has been investigated for effects on acute tissue injury, with promising results (Assmus et al., 2002; Tateishi-Yuyama et al., 2002). BM-MNC transplantation via the CSF after SCI has several advantages over other kinds of cell therapies, including those that use neural stem cells or embryonic stem cells. Furthermore, although transplantation of embryonic stem cells and neural precursor cells is reported to induce recovery from SCI (McDonald et al., 1999; Ogawa et al., 2002), some unresolved critical issues (i.e., ethical concerns and immunosuppression) have prevented its clinical application.

Clinical transplantation of BM-MNC via the CSF may be realized earlier than transplantation of these other types of cells. BM-MNC are easily collected and can be transplanted at the most appropriate time after SCI without sacrificing the time window critical for a therapeutic effect, and there is no need to expand BM-MNC by culture to obtain a sufficient number of cells for transplantation. Moreover, in the clinical setting, BM-MNC can be transplanted via the CSF by means of lumbar puncture rather than having to be given by ventricular injection, thereby reducing the risk of additional injury to intact spinal cord at the injury site.

In conclusion, transplantation of BM-MNC after SCI has a remarkable neuroprotective effect in the acute stage of injury, suppresses cavity formation, and contributes to functional recovery. Our observations provide evidence that clinical administration of BM-MNC can play a critical role in neuroprotection and new vessel formation for functional recovery after SCI, and we conclude that transplantation of BM-MNC after SCI is a potentially effective means of enhancing functional recovery from such injury.

ACKNOWLEDGMENTS

We are grateful to Associate Professors Hiroshi Tanaka and Takeshi Shimazu for their helpful advice, and we thank all of the members of our laboratory for critical discussion pertaining to the experiments done in the present study. This work was supported in part by the Ministry of Education, Science, Sports and Culture of Japan (grant 15300114), and the Ministry of Health, Labour and Welfare of Japan (grant 16C-7, H18-Kokoro-024).

REFERENCES

ASSMUS, B., SCHACHINGER, V., TEUPE, C., et al. (2002). Transplantation of progenitor cells and regeneration enhancement in acute myocardial infarction (TOPCARE-AMI). Circulation **106,** 3009–3017.

AZIZI, S.A., STOKES, D., AUGELLI, B.J., et al. (1998). Engraftment and migration of human bone marrow stromal cells implanted in the brains of albino rats—similarities to astrocyte grafts. Proc. Natl. Acad. Sci. USA **95,** 3908–3913.

BAI, H., SUZUKI, Y., NODA, T., et al. (2003). Dissemination and proliferation of neural stem cells on the spinal cord by injection into the fourth ventricle of the rat: a method for cell transplantation. J. Neurosci. Methods **124,** 181–187.

BASSO, D.M., BEATTIE, M.S., and BRESNAHAN, J.C. (1995). A sensitive and reliable locomotor rating scale for open field testing in rats. J. Neurotrauma **12,** 1–21.

CARMELIET, P. (2003). Angiogenesis in health and disease. Nat. Med. **9,** 653–660.

CHEN, X., KATAKOWSKI, M., LI, Y., et al. (2002). Human bone marrow stromal cell cultures conditioned by traumatic brain tissue extracts: growth factor production. J. Neurosci. Res. **69,** 687–691.

DOUCETTE, R. (1995). Olfactory ensheathing cells: potential for glial cell transplantation into areas of CNS injury. Histol. Histopathol. **10,** 503–507.

FITCH, M.T., DOLLER, C., COMBS, C.K., et al. (1999). Cellular and molecular mechanisms of glial scarring and progressive cavitation: *in vivo* and *in vitro* analysis of inflammation-induced secondary injury after CNS trauma. J. Neurosci. **19,** 8182–8198.

GIULIAN, D., CHEN, J., INGEMAN, J.E., GEORGE, J.K., and NOPONEN, M. (1989). The role of mononuclear phagocytes in wound healing after traumatic injury to adult mammalian brain. J. Neurosci. **9,** 4416–4429.

IDE, C., KITADA, M., CHAKRABORTTY, S., et al. (2001). Grafting of choroid plexus ependymal cells promotes the growth of regenerating axons in the dorsal funiculus of rat spinal cord: a preliminary report. Exp. Neurol. **167,** 242–251.

IMPERATO-KALMAR, E.L., McKINNEY, R.A., SCHNELL, L., et al. (1997). Local changes in vascular architecture following partial spinal cord lesion in the rat. Exp. Neurol. **145,** 322–328.

KAMIHATA, H., MATSUBARA, H., NISHIUE, T., et al. (2001). Implantation of bone marrow mononuclear cells into ischemic myocardium enhances collateral perfusion and regional function via side supply of angioblasts, angiogenic ligands, and cytokines. Circulation **104,** 1046–1052.

KONDZIOLKA, D., WECHSLER, L., GOLDSTEIN, S., et al. (2000). Transplantation of cultured human neuronal cells for patients with stroke. Neurology **55,** 565–569.

KOSHIZUKA, S., OKADA, S., OKAWA, A., et al. (2004). Transplanted hematopoietic stem cells from bone marrow differentiate into neural lineage cells and promote functional recovery after spinal cord injury in mice. J. Neuropathol. Exp. Neurol. **63,** 64–72.

LINDVALL, O., and KOKAIA, Z. (2004). Recovery and rehabilitation in stroke: stem cells. Stroke **35,** 2691–2694.

LIU, Y., GUO, J., ZHANG, P., et al. (2004). Bone marrow mononuclear cell transplantation into heart elevates the expression of angiogenic factors. Microvasc. Res. **68,** 156–160.

MARTIN, D., ROBE, P., FRANZEN, R., et al. (1996). Effects of Schwann cell transplantation in a contusion model of rat spinal cord injury. J. Neurosci. Res. **45,** 588–597.

McDONALD, J.W., LIU, X.Z., QU, Y., et al. (1999). Transplanted embryonic stem cells survive, differentiate and promote recovery in injured rat spinal cord. Nat. Med. **5,** 1410–1412.

OGAWA, Y., SAWAMOTO, K., MIYATA, T., et al. (2002). Transplantation of *in vitro*-expanded fetal neural progenitor cells results in neurogenesis and functional recovery after spinal cord contusion injury in adult rats. J. Neurosci. Res. **69,** 925–933.

OHTA, M., SUZUKI, Y., NODA, T., et al. (2004). Bone marrow stromal cells infused into the cerebrospinal fluid promote functional recovery of the injured rat spinal cord with reduced cavity formation. Exp. Neurol. **187,** 266–278.

REHMAN, J., LI, J., ORSCHELL, C.M., and MARCH, K.L. (2003). Peripheral blood "endothelial progenitor cells" are derived from monocyte/macrophages and secrete angiogenic growth factors. Circulation **107,** 1164–1169.

REYES, M., and VERFAILLIE, C.M. (2001). Characterization of multipotent adult progenitor cells, a subpopulation of mesenchymal stem cells. Ann. N.Y. Acad. Sci. **938,** 231–235.

SHINTANI, S., MUROHARA, T., IKEDA, H., et al. (2001). Augmentation of postnatal neovascularization with autologous bone marrow transplantation. Circulation **103,** 897–903.

STRAUER, B.E., BREHM, M., ZEUS, T., et al. (2002). Repair of infarcted myocardium by autologous intracoronary mononuclear bone marrow cell transplantation in humans. Circulation **106,** 1913–1918.

TAGUCHI, A., SOMA, T., TANAKA, H., et al. (2004). Administration of $CD34^+$ cells after stroke enhances neurogenesis via angiogenesis in a mouse model. J. Clin. Invest. **114,** 330–338.

TAKAMI, T., OUDEGA, M., BETHEA, J.R., et al. (2002). Methylprednisolone and interleukin-10 reduce gray matter damage in the contused Fischer rat thoracic spinal cord but do not improve functional outcome. J. Neurotrauma **19,** 653–666.

TATEISHI-YUYAMA, E., MATSUBARA, H., MUROHARA, T., et al. (2002). Therapeutic angiogenesis for patients with limb ischaemia by autologous transplantation of bone-marrow cells: a pilot study and a randomised controlled trial. Lancet **360,** 427–435.

TOMITA, M., ADACHI, Y., YAMADA, H., et al. (2002). Bone marrow–derived stem cells can differentiate into retinal cells in injured rat retina. Stem Cells **20,** 279–283.

TSUZUKI, N., MIYAZAWA, T., MATSUMOTO, K., et al. (2000). Hepatocyte growth factor reduces infarct volume after transient focal cerebral ischemia in rats. Acta Neurochir. Suppl. **76,** 311–316.

VALABLE, S., BELLAIL, A., LESNE, S., et al. (2003). Angiopoietin-1–induced PI3-kinase activation prevents neuronal apoptosis. FASEB J. **17,** 443–445.

WIDENFALK, J., LIPSON, A., JUBRAN, M., et al. (2003). Vascular endothelial growth factor improves functional outcome and decreases secondary degeneration in experimental spinal cord contusion injury. Neuroscience **120,** 951–960.

WU, S., SUZUKI, Y., EJIRI, Y., et al. (2003). Bone marrow stromal cells enhance differentiation of cocultured neurosphere cells and promote regeneration of injured spinal cord. J. Neurosci. Res. **72,** 343–351.

ZHANG, Z., and GUTH, L. (1997). Experimental spinal cord injury: Wallerian degeneration in the dorsal column is followed by revascularization, glial proliferation, and nerve regeneration. Exp. Neurol. **147,** 159–171.

ZHANG, L., HIMI, T., MORITA, I., and MUROTA, S. (2000). Hepatocyte growth factor protects cultured rat cerebellar granule neurons from apoptosis via the phosphatidylinositol-3 kinase/Akt pathway. J. Neurosci. Res. **59,** 489–496.

Address reprint requests to:
Tomoyuki Yoshihara, M.D.
Department of Traumatology
and Acute Critical Medicine
Osaka University Graduate School of Medicine
2-15 Yamadaoka, Suita
Osaka 565-0871, Japan

E-mail: t-yoshihara@umin.ac.jp

Available online at www.sciencedirect.com
ScienceDirect
Biochemical and Biophysical Research Communications 359 (2007) 915–920
BBRC
www.elsevier.com/locate/ybbrc

Peripheral nerve regeneration by the in vitro differentiated-human bone marrow stromal cells with Schwann cell property

Satoshi Shimizu, Masaaki Kitada, Hiroto Ishikawa, Yutaka Itokazu, Shohei Wakao, Mari Dezawa *

Department of Anatomy and Neurobiology, Kyoto University Graduate School of Medicine, Yoshida-Konoecho, Sakyo-ku, Kyoto 606-8501, Japan

Received 20 May 2007
Available online 8 June 2007

Abstract

We examined the availability of human bone marrow stromal cells (MSCs) as a source of transplantation therapy in nerve injury. Human MSCs were subjected to a series of treatments with a reducing agent, retinoic acid and a combination of trophic factors. Morphologically and immunocytochemically, such treated cells differentiated into Schwann cell characteristics in vitro. Cells were filled into a transpermeable tube, transplanted into the gap made in the rat sciatic nerve of a rat and followed up to 3 weeks under the control of immunosuppressant. In contrast to untreated human MSCs, differentiated human MSCs expressed Schwann cell markers in vivo and supported regenerating axons. These results suggest that human MSCs can be induced to be a substitute for Schwann cells that may be applied for nerve regeneration.
© 2007 Elsevier Inc. All rights reserved.

Keywords: Cell therapy; Human mesenchymal cells; Transdifferentiation; Schwann cells; Transplantation; Peripheral nerve injury; Reconstruction

Schwann cells are peripheral glial cells that ensheath axons to form myelin in the peripheral nervous system (PNS). Following nerve injury, Schwann cells lose myelin, are activated, and proliferate within the distal nerve segment to produce a variety of neurotrophic factors, cytokines, and cell adhesion molecules thereby providing the pathway for regenerating axons. This process is collectively called Wallerian degeneration [1–3]. Schwann cells also play a crucial role in the endogenous repair of PNS by reconstructing myelin which is indispensable for nerve function. They are also known to support reconstruction of the injured central nervous system (CNS) where successful axonal regeneration and functional reconstruction do not normally occur. Several experiments in the spinal cord and some other areas in the CNS have shown that either the injection or transplantation of the polymer tube filled with cultured Schwann cells improved axonal growth across the site of injury [4–8]. For these reasons, they are one of the most widely studied cell types for the axonal regeneration both in PNS and CNS.

Even though cell-based therapy using Schwann cells seems to be effective and promising for the treatment of neurotraumatic injuries and neurodegenerative diseases, another peripheral nerve must be sacrificed for the cultivation of Schwann cells. Furthermore, technical difficulties exist in the harvesting and expansion of Schwann cells to obtain sufficient amount of cells for cell-based therapy within a reasonable time period. Therefore, it is desirable to harvest the highly proliferative cells from easily accessible sources other than PNS to produce the cells with Schwann cell characteristics.

Bone marrow stromal cells (MSCs) are mesenchymal elements normally providing structural and functional support for hemopoiesis [9,10]. The great benefits of MSCs are that they are easily accessible through aspiration of the bone marrow from patients without serious ethical problems, and can be readily expanded in large scale for

* Corresponding author. Fax: +81 75 751 7286.
E-mail address: dezawa@anat2.med.kyoto-u.ac.jp (M. Dezawa).

0006-291X/$ - see front matter © 2007 Elsevier Inc. All rights reserved.
doi:10.1016/j.bbrc.2007.05.212

autotransplantation. They are known to have the potential to differentiate into other kinds of cells such as osteoblasts, adipocytes, and chondrocytes [11].

The main purpose of this study is to verify the possibility of human MSCs to transdifferentiate into cells with Schwann cell property and to explore their function after grafting. We show the induction of human MSCs into Schwann-like cells in vitro and their *involvement in the axonal* regeneration in vivo. Thus this induction system is expected to serve human MSCs alternative to Schwann cells that may be applied for auto-cell-transplantation therapy in nerve injury.

Materials and methods

Cell culture. The usage of human MSCs for the experiment was approved by Kyoto University Graduate School and Faculty of Medicine, Ethics Committee. All animal experiments were approved by the Animal Care and Experimentation Committee of Kyoto University Graduate School of Medicine. Human MSCs were purchased from Cambrex (East Rutherford, NJ) and were cultured in alpha-minimum essential medium (α-MEM) (Sigma, St. Louis, MO) containing 10% fetal bovine serum (FBS) and kanamycin at 37 °C, 5% CO_2. Rat MSCs were harvested according to the former study [12]. Primary rat MSCs were isolated from the tibias and femurs of 12-week-old male Wistar rats. The marrow was extruded in α-MEM with 15% FBS, 2 mM L-glutamine, and kanamycin, and incubated at 37 °C, 5% CO_2. After 48 h, the non-adherent cells were removed by replacing the medium. MSCs were subcultured four times and finally subjected to induction. Rat Schwann cell-line was commercially obtained from American Type Culture Collection (ATCC; Manassas, VA).

The induction of M-Schwann cells. After subculturing at the concentration of 1.27×10^3 cells/cm^2, MSCs were incubated in α-MEM containing 1 mM beta-mercaptoethanol (β-ME) without serum for 24 h. The culture media was then replaced with α-MEM containing 10% FBS and 35 ng/ml all-*trans*-retinoic acid (ATRA) (Sigma, St. Louis, MO). Three days later, cells were finally transferred to α-MEM containing 10% FBS and trophic factors of 5 μM forskolin (Calbiochem, La Jolla, CA), 10 ng/ml recombinant human basic fibroblast growth factor (Peprotech, London, UK), 5 ng/ml platelet-derived growth factor-AA (Peprotech, London, UK), and 200 ng/ml heregulin-β1-EGF-domain (R&D systems Minneapolis, MN) and cultured for 4–5 days. These treated MSCs were referred to as M-Schwann cells in the following text.

Evaluation of M-Schwann cells. M-Schwann cells were evaluated both by phase-contrast microscopic observation and immunocytochemistry. For immunocytochemistry, human MSCs and M-Schwann cells, and rat Schwann cell-line were fixed with 4% paraformaldehyde in 0.01 M phosphate-buffered saline (PBS). Primary antibodies used for immunocytochemistry were anti-S100 rabbit IgG (1:200, DAKO, Carpinteria, CA), anti-P0 rabbit IgG (1:300, kindly provided by Dr. J.J. Archelos, Karl-Franzens Universitat, Graz, Austria), anti-p75NGF receptor mouse IgG (1:500, Abcam Cambridge, UK), anti-Glial Fibrillary Acidic Protein (GFAP) rabbit IgG (1:300, DAKO Carpinteria, CA), anti-L1 mouse IgG (1:100, kindly provided by Dr. Fritz Rathejen, Zentrum für Molekulare Neurobiologie, Hamburg), and anti-O4 mouse IgM (1:20, Boehringer Ingelheim GmbH, Ingelheim, Germany) antibodies, and were detected by Alexa568 conjugated anti-rabbit IgG, anti-mouse IgG or anti-mouse IgM antibodies (Molecular Probes, Invitrogen, Eugene, OR). Samples were incubated in 20% BlockAce (skim milk, Yukijirushi, Tokyo, Japan) in 0.005% saponin and 50 mM glycine in PBS (SaGlyPBS) for 10 min, incubated with the primary antibody in 5% BlockAce in SaGlyPBS overnight at 4 °C followed by the secondary antibody incubation in 5% BlockAce in SaGlyPBS. Nuclei were counter-stained with 4′,6-diamidino-2-phenylindole (DAPI). All images were taken by a confocal laser scanning microscope (CS-1, Nikon, Kawasaki, Japan) in the same laser intensity and detection sensitivity.

Transplantation of cells into rat sciatic nerve injury. Prior to transplantation, both human MSCs (untreated) and human M-Schwann cells were infected with the lentivirus-green fluorescent protein (GFP) (provided by Dr. D. Trono) to label the cells as described [13], and confirmed under fluorescence microscopy that more than 95% of MSCs or M-Schwann cells expressed GFP.

Human MSCs or M-Schwann cells were suspended in matrigel (BD Biosciences, Bedford, MA) at the concentration of $1–2 \times 10^7$ cells/ml, and were filled into trans-permeable tubes (Hollow fibers, Amicon, Beverly, MA) (10 mm length) to make an artificial graft. Under general anesthesia with halothane, a 10-mm segment was completely removed from the left side of the sciatic nerve of 8-week-old male Wistar rats at the middle of the thigh. The artificial graft was anastomosed with proximal and distal nerve tips using 10-0 nylon sutures at both ends. To avoid immunorejection, intraperitoneal administration of FK506 (Fujisawa Pharmaceutical Co. Ltd., Osaka, Japan) was performed at 0.05 mg/kg every day for the first 2 weeks and every other day for the third week.

Walking track analysis. Three weeks after transplantation, walking track analysis, one of the behavioral analyses for estimation of functional recovery from the sciatic nerve injury, was performed according to the protocol reported in the past studies [14,15]. The rat's hind feet were dipped in China ink and animals were permitted to walk on a sheet of paper along a tunnel. The lengths of the third toe to its heel (PL), the first to the fifth toe (TS), and the second toe to the fourth toe (ITS) were measured with their footprints of both MSCs- and M-Schwann cells-transplanted groups. The Sciatic Function Index (SFI) in each animal was calculated by the specific formula below:

$$SFI = -38.3 \times (PLe - PLn)/PLn + 109.5 \times (TSe - TSn)/TSn + 13.3 \times (ITSe - ITSn)/ITSn - 8.8$$

(e, experimental side; n, normal side).

This index has been found to be both reproducible and of high sensitivity for detecting nerve dysfunction [14,15].

Immunohistochemical analysis of transplanted grafts. After completing walking track analysis, animals (3 weeks after transplantation) were sacrificed by an overdose of diethyl ether and perfused transcardially with periodate–lysine–paraformaldehyde fixative. The left sciatic nerve including the graft was dissected and incubated in the same fixative for 6 h at 4 °C. Tissues were washed with 0.1 M PBS overnight at 4 °C, immersed in 10%, 20%, and 30% sucrose–PBS for 3 h each at 4 °C, embedded in OCT, and cut into 10-μm-thick frozen sections by a cryostat. Primary antibodies used for immunohistochemistry were anti-neurofilament (NF) mouse IgG (1:50, Sigma, St. Louis, MO), anti-myelin-associated glycoprotein (MAG) mouse IgG (1:50, Boehringer Ingelheim), and anti-myelin basic protein (MBP) (1:500, Boehringer Ingelheim). Secondary antibodies were anti-rabbit IgG goat, mouse IgG goat or anti-mouse IgM goat antibodies conjugated to Alexa568 (Molecular Probes). The ratio of GFP-positive-transplanted cells to cells positive to MAG (including both host Schwann cells and transplanted cells) with elongated morphology was counted in a high magnification (400×) within the graft ($n = 4$).

Results

Characterization of induced human M-Schwann cells

Phase-contrast microscopic observation showed the morphological changes of human MSCs during the process of induction (Fig. 1A–D). Untreated human MSCs exhibited the fibroblast-like morphology (Fig. 1A), as was similarly reported in MSCs of other species [16], while after the trophic factor treatment, MSCs finally changed into the spindle-shaped smaller cells (Fig. 1D). We have previously reported in the rat MSCs that, after treatment with the same induction protocol, differenti-

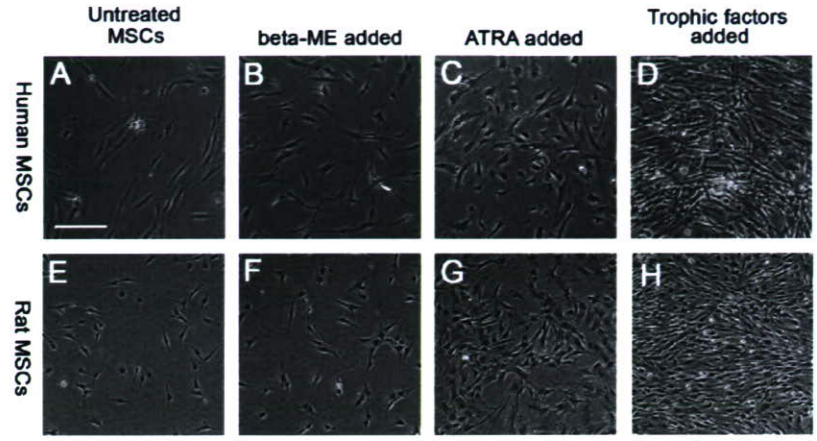

Fig. 1. Phase-contrast microscopic observation showing morphological changes of human MSCs (A–D) and rat MSCs (E–H) during the induction. The original MSCs presented the fibroblast-like morphology (A in human, E in rat). As the induction protocol proceeds, MSCs changed to spindle-shape (D in human, H in rat). Scale bar, 250 μm.

ated MSCs were morphologically different from the original MSCs but resembled to Schwann cells derived from dorsal root ganglion and contributed to nerve regeneration and myelin reconstruction when transplanted into the injured PNS [17,18], spinal cord injury [19]. We reproduced this rat MSC experiment in this study (Fig. 1E and H) and confirmed that the rat M-Schwann cells are similar to rat Schwann cells derived from dorsal root ganglion as described (data not shown) [17]. We also compared the human MSCs system to that of the rat system, and recognized that even though the cell size of rat MSCs were smaller than those of human MSCs, the induction process was similar in both cell types (Fig. 1A–H). Immunocytochemical analysis showed that the untreated human MSCs were initially negative for Schwann cell markers of P0, p75NGF receptor, GFAP, L1, and O4 but with slight positivity for S100 (Fig. 2A–F). After the induction, human M-Schwann cells became positive for markers of P0, p75NGF receptor, GFAP, and L1 with the increased immuno-positivity to S100 (Fig. 2G–L). Positive control experiments for all these markers were performed in rat Schwann cell-line (Fig. 2M–R).

Morphological assessment of the grafts

The grafts were well connected with the host peripheral nerve tissue in both the human MSC-transplanted (MSC-group) and the human M-Schwann cell-transplanted (M-Schwann group) rat sciatic nerves. Anastomosis between the graft and host sciatic nerve segments remained tight, and the site of anastomosis in each graft was covered by connective tissue. Within the graft, newly formed whitish parenchymatous tissue was observed in both groups for the entire length of the graft, but the tissue of the M-Schwann group was thicker and more robust than that of the MSC-group which was fragile and weaker against tension (Fig. 3A and B).

Immunohistochemistry to NF clearly showed that a large number of regenerating axons elongated into the graft in the M-Schwann group. Additionally, some of the regenerating nerve fibers successfully reached the distal nerve segment (Fig. 3C). On the other hand, few regenerating nerve fibers were observed to cross the proximal segment that reached the graft in the MSC-group (Fig. 3D).

In the M-Schwann cell transplanted animals, nuclei of the GFP-positive transplanted cells were in elliptical shape similar to host Schwann cells, and green fluorescence of the grafted cells was typically observed as elongated in both sides, suggesting spindle-shaped morphology of the grafted cells (Fig. 4). The ratio of GFP-positive cells was only as much as $12.6 \pm 2.98\%$ among all MAG-positive cells within the graft ($n = 4$). 3D-constructed images revealed that some transplanted cells covered the regenerating axons (Fig. 4A), and expressed MAG (Fig. 4B–D) and MBP (Fig. 4E–G) with the staining intensity that was equal to or slightly weaker than that of endogenous Schwann cells.

In the case of the MSC-group, regeneration of nerve fibers was scant as described above. Phagocytosed human MSCs detected as GFP-positive-cell debris were frequently observed throughout the grafts, and neither contact between the nerve fiber and GFP-positive transplanted cells nor expression of Schwann cell markers could be recognized (data not shown). In addition, regenerating axons and endogenous Schwann cells were extremely limited (data not shown).

Walking track analysis

SFI in the normal rat is of the range -1.9 ± 6.3 [14]. The number of SFI was -85.52 ± 2.1 in the M-Schwann group and -79.12 ± 2.1 in the MSC-group, respectively. There was statistical difference between these indices ($p = 0.047$), indicating that the M-Schwann group exhibited if not outstanding but better, functional improvement than the case of MSC-group.

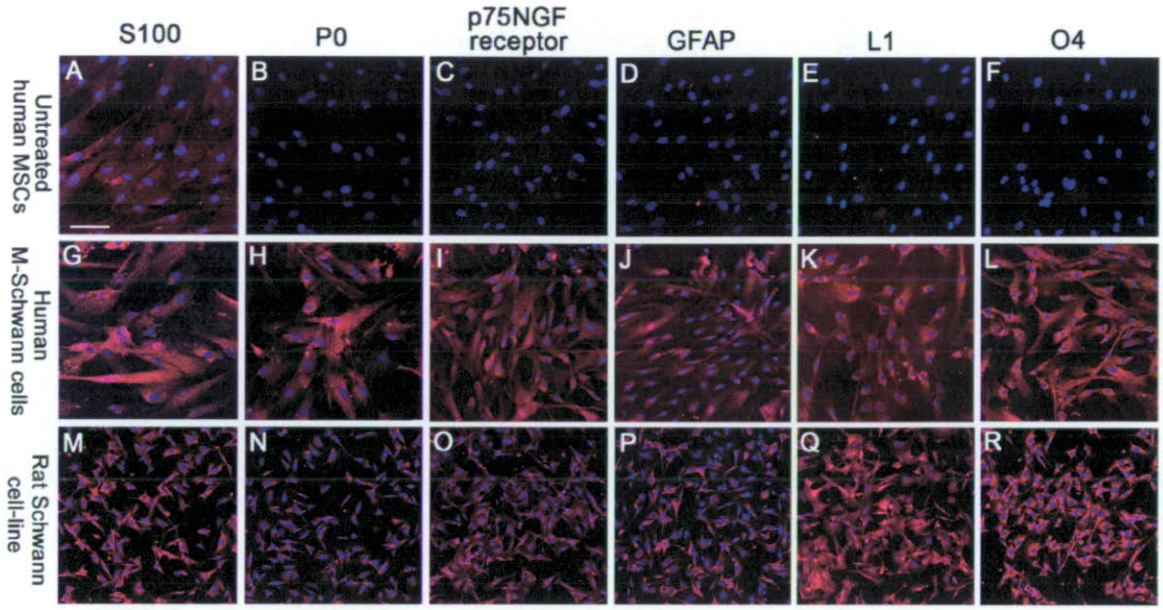

Fig. 2. Immunocytochemistry of S100 (A,G,M), P0 (B,H,N), p75NGFR (C,I,O), GFAP (D,J,P), L1 (E,K,Q), O4 (F,L,R) in human MSCs (A–F), human M-Schwann cells (G–L), and rat Schwann cell-line (M–R). The untreated human MSCs slightly expressed S100 (A) but were negative for other Schwann cell markers (B–F). After the induction, M-Schwann cells became positive for P0 (H), p75NGFR (I), GFAP (J), L1 (K), O4 antigen (L) and the immunoreactivity for S100 was upregulated (G). Rat Schwann cell-line was used as positive control for all these Schwann cell markers (M–R). Scale bar, 100 μm.

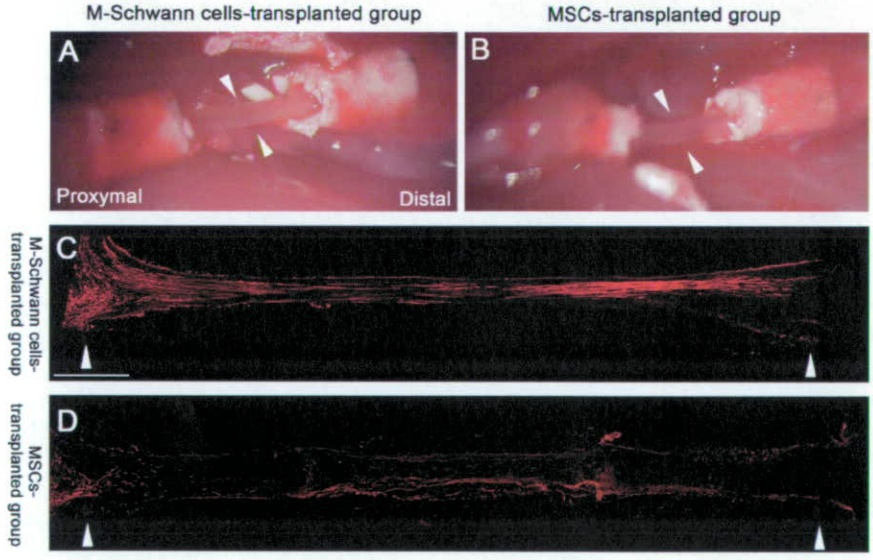

Fig. 3. Macroscopic observation of the parenchymatous tissue within the graft of M-Schwann (A) and MSC (B) groups 3 weeks after transplantation. The newly formed tissue was seen in both groups (arrowheads). The proximal segment (left) and the distal segment (right) of the sciatic nerve were indicated. Neurofilament-positive nerve fibers (red color-coded) observed in MSC (C) and M-Schwann (D) groups. Many regenerating nerve fibers were observed to enter into the graft from the proximal segment (left) and reached the distal nerve segment (right) in the M-Schwann cells-transplanted group (D). In contrast, regenerating nerve fibers were scarcely observed around the proximal segment and within the graft (D). Arrowheads showed the proximal and the distal edges of the grafts. Scale bar in C and D, 100 μm. (For interpretation of the references to color in this figure legend, the reader is referred to the web version of this paper.)

Discussion

This study showed a series of treatments with β-ME followed by retinoic acid and a certain combination of trophic factors was able to induce the differentiation of human MSCs into cells with Schwann cell characteristics which are able to support PNS regeneration in vivo. Notably, this induction system could be achieved without gene introduc-

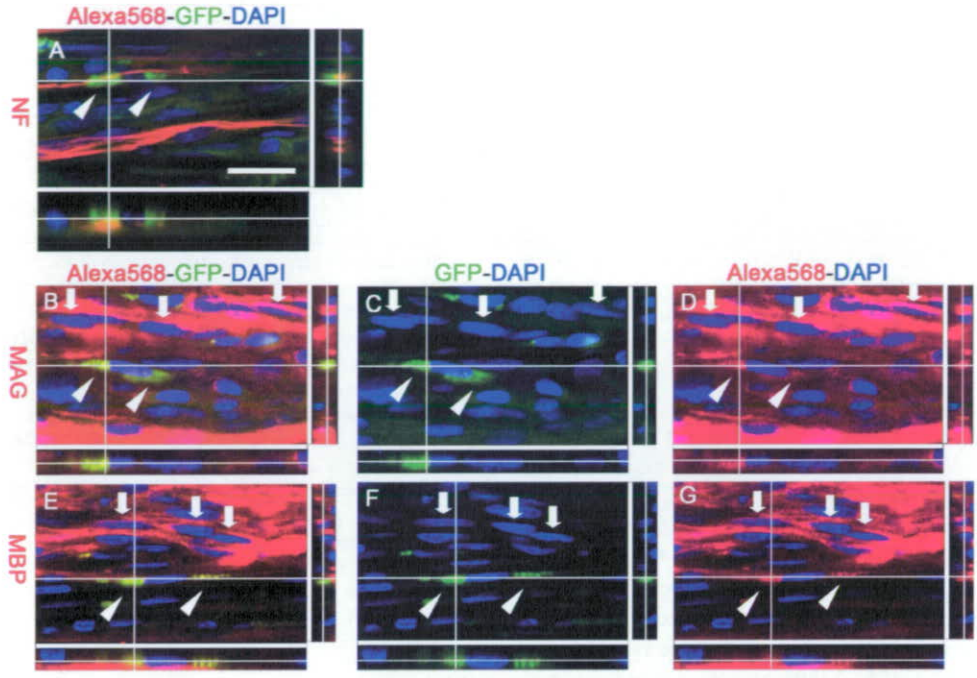

Fig. 4. Immunohistochemistry of the grafts 3 weeks after operation in the M-Schwann group. Transplanted cells were visualized by its expression of GFP (green). (A) The GFP-positive transplanted cells were found to cover the regenerating nerve fiber in the 3D-constructed image as revealed by immunostaining against NF (red). (B–G) The GFP-positive human M-Schwann cells (arrowheads) expressed MAG (red in B–D) and MBP (red in E–G). Endogenous host Schwann cells (arrows), also observed in the graft, expressed MAG (red in B–D) and MBP (red in E–G). Scale bar, 20 μm. (For interpretation of the references to color in this figure legend, the reader is referred to the web version of this paper.)

tion but simply by the administration of chemical reagents and trophic factors. This is beneficial to the safety improvement for cell-based therapy. The use of FBS during the culture and induction will be another problem for safety. Therefore, we estimated whether human serum was available for this system, and confirmed that all data shown in this study was reproducible (data not shown). This is remarkable from the point of view that auto-cell transplantation therapy in that patient's own serum and MSCs could be used for the induction of Schwann cell characteristics that will be applied for cell-based therapy of nerve regeneration.

It was noteworthy that the transplanted human GFP-positive M-Schwann cells were in close contact with NF-positive regenerating axons, and those M-Schwann cells expressed myelin-associated markers of MAG and MBP. These findings suggest that, not only in vitro, human M-Schwann cells retained their characteristics similar to Schwann cells even after transplantation, thereby also supported axonal regeneration if not strongly. However, there remains the question whether these transplanted human M-Schwann cells are able to reconstruct multilamellar myelin within the graft. For further evaluation, we subjected sections observed in immunohistochemistry to the immunoelectronmicroscopic observation. Even though the close contacts between anti-GFP-labeled transplanted M-Schwann cells and the regenerating axons could be observed, remyelination of the regenerating axons by those transplanted cells was not apparent (data not shown). Actually, it is a well-known fact that remyelination requires longer duration in the regeneration procedure, and 3 weeks is the point when remyelination starts in the normal PNS regeneration. This may be one of the reasons why remyelination by human M-Schwann cells could not be clearly recognized. In this study, immunorejection to human cells was controlled by FK506. Thus, there was a limit for a longer period of observation because the additional dose of FK506 would have lead to death or infectious diseases in transplanted animals. The second possibility is that the control of immunorejection by FK506 should not be perfect. In fact, GFP-positive cell-debris could occasionally be recognized even in the M-Schwann group (data not shown), so that remyelinating human M-Schwann cells might have disappeared by phagocytosis to some extent. In the MSC-group, in which phagocytosis of GFP-positive cell was prominent, regenerating axons as well as endogenous (host-derived) Schwann cells were observed far less than those in the M-Schwann group. These findings suggest that immunorejection caused the alteration of tissue environment which is not permissive for the nerve regeneration. Thirdly, another factor that may influence on the observation of remyelination would be the direct effect of FK506 on nerve regeneration [20,21]. We have previously reported the improvement of motor function, electrophysiological data, and myelin reconstruction in rat PNS regeneration up to 6 months after transplantation of rat M-Schwann

cells [18]. From the result obtained in this study, human M-Schwann cells are expected to possess Schwann cell property. However, the final answer could be obtained by the precise analysis using primate experiments.

Walking track analysis was performed to estimate the extent of functional recovery of the sciatic nerve to find statistical difference between M-Schwann cells- and MSCs-transplanted groups. However, the SFI of the M-Schwann cells-transplanted group was only -79.12 ± 2.1. This data correlate with the fact that the ratio of GFP-positive cells among MAG-positive cells were not so high, suggesting that the number (namely, the contribution) of transplanted human M-Schwann cell was not large enough for supporting the functional recovery. This may be partly because the immunorejection of transplanted M-Schwann cells lowered the efficiency of cell therapy for nerve regeneration. On the other hand, we have previously shown that rat M-Schwann cells supported significant recovery in walking track analysis 6 months after transplantation into PNS [18]. Again, appropriate methods to prevent immunological rejection will give the best effect of human Schwann cells in clinical use.

There remain some points to be clarified or resolved for the clinical application of M-Schwann cells as the source of cell-based therapy. For example, as both MSCs and M-Schwann cells are highly proliferative in vitro, the risk of tumorigenesis has to be carefully evaluated in the longer observations. The possibility has been reported that human MSCs might undergo spontaneous transformation following long-term in vitro culture [22,23]. Biosafety studies of MSCs are required at least in these regards. Furthermore, for the future clinical use, the graft should be carefully designed and brushed up by combining the technology developed in tissue engineering such as matrix and foothold that may support survival and differentiation of transplanted cells in the host. We hope that our report will contribute to bring one of the solutions to the cell therapy designed for the regeneration of PNS and CNS.

Acknowledgements

This study was supported by the Program for Promotion of Fundamental Studies in Health Sciences of the National Institute of Biomedical Innovation (NIBIO, #05-6) and by The Research on Psychiatric and Neurological Disease and Mental Health (H19-016).

References

[1] J.W. Fawcett, R.J. Keynes, Peripheral nerve regeneration, Annu. Rev. Neurosci. 13 (1990) 43–60.
[2] K. Torigoe, H.F. Tanaka, A. Takahashi, A. Awaya, K. Hashimoto, Basic behavior of migratory Schwann cells in peripheral nerve regeneration, Exp. Neurol. 137 (1996) 301–308.
[3] S. Hall, Nerve repair: a neurobiologist's view, J. Hand Surg. [Br] 26 (2001) 129–136.
[4] M.B. Bunge, Transplantation of purified populations of Schwann cells into lesioned adult rat spinal cord, J. Neurol. 242 (1994) S36–S39.
[5] A.R. Harvey, G.W. Plant, Schwann cells and fetal tectal tissue cografted to the midbrain of newborn rats: fate of Schwann cells and their influence on host retinal innervation of grafts, Exp. Neurol. 134 (1995) 179–191.
[6] A.R. Harvey, G.W. Plant, M.M. Tan, Schwann cells and the regrowth of axons in the mammalian CNS: a review of transplantation studies in the rat visual system, Clin. Exp. Pharmacol. Physiol. 22 (1995) 569–579.
[7] H. Negishi, M. Dezawa, T. Oshitari, E. Adachi-Usami, Optic nerve regeneration within artificial Schwann cell graft in the adult rat, Brain Res. Bull. 55 (2001) 409–419.
[8] M. Oudega, S.E. Gautier, P. Chapon, M. Fragoso, M.L. Bates, J.M. Parel, M.B. Bunge, Axonal regeneration into Schwann cell grafts within resorbable poly(alpha-hydroxyacid) guidance channels in the adult rat spinal cord, Biomaterials 22 (2001) 1125–1136.
[9] M.F. Pittenger, A.M. Mackay, S.C. Beck, R.K. Jaiswal, R. Douglas, J.D. Mosca, M.A. Moorman, D.W. Simonetti, S. Craig, D.R. Marshak, Multilineage potential of adult human mesenchymal stem cells, Science 284 (1999) 143–147.
[10] M.F. Pittenger, J.D. Mosca, K.R. McIntosh, Human mesenchymal stem cells: progenitor cells for cartilage, bone, fat and stroma, Curr. Top. Microbiol. Immunol. 251 (2000) 3–11.
[11] D.J. Prockop, Marrow stromal cells as stem cells for nonhematopoietic tissues, Science 276 (1997) 71–74.
[12] S.A. Azizi, D. Stokes, B.J. Augelli, C. DiGirolamo, D.J. Prockop, Engraftment and migration of human bone marrow stromal cells implanted in the brains of albino rats—similarities to astrocyte grafts, Proc. Natl. Acad. Sci. USA 95 (1998) 3908–3913.
[13] T.H. Nguyen, T. Khakhoulina, A. Simmons, P. Morel, D. Trono, A simple and highly effective method for the stable transduction of uncultured porcine hepatocytes using lentiviral vector, Cell Transplant. 14 (2005) 489–496.
[14] J.R. Bain, S.E. Mackinnon, D.A. Hunter, Functional evaluation of complete sciatic, peroneal, and posterior tibial nerve lesions in the rat, Plast. Reconstr. Surg. 83 (1989) 129–138.
[15] G.M. Hare, P.J. Evans, S.E. Mackinnon, T.J. Best, J.R. Bain, J.P. Szalai, D.A. Hunter, Walking track analysis: a long-term assessment of peripheral nerve recovery, Plast. Reconstr. Surg. 89 (1992) 251–258.
[16] G.C. Kopen, D.J. Prockop, D.G. Phinney, Marrow stromal cells migrate throughout forebrain and cerebellum, and they differentiate into astrocytes after injection into neonatal mouse brains, Proc. Natl. Acad. Sci. USA 96 (1999) 10711–10716.
[17] M. Dezawa, I. Takahashi, M. Esaki, M. Takano, H. Sawada, Sciatic nerve regeneration in rats induced by transplantation of in vitro differentiated bone-marrow stromal cells, Eur. J. Neurosci. 14 (2001) 1771–1776.
[18] T. Mimura, M. Dezawa, H. Kanno, H. Sawada, I. Yamamoto, Peripheral nerve regeneration by transplantation of bone marrow stromal cell-derived Schwann cells in adult rats, J. Neurosurg. 101 (2004) 806–812.
[19] T. Kamada, M. Koda, M. Dezawa, K. Yoshinaga, M. Hashimoto, S. Koshizuka, Y. Nishio, H. Moriya, M. Yamazaki, Transplantation of bone marrow stromal cell-derived Schwann cells promotes axonal regeneration and functional recovery after complete transection of adult rat spinal cord, J. Neuropathol. Exp. Neurol. 64 (2005) 37–45.
[20] B.G. Gold, K. Katoh, T. Storm-Dickerson, The immunosuppressant FK506 increases the rate of axonal regeneration in rat sciatic nerve, J. Neurosci. 15 (1995) 7509–7516.
[21] M.S. Wang, M. Zeleny-Pooley, B.G. Gold, Comparative dose-dependence study of FK506 and cyclosporin A on the rate of axonal regeneration in the rat sciatic nerve, J. Pharmacol. Exp. Ther. 282 (1997) 1084–1093.
[22] N. Serakinci, P. Guldberg, J.S. Burns, B. Abdallah, H. Schrodder, T. Jensen, M. Kassem, Adult human mesenchymal stem cell as a target for neoplastic transformation, Oncogene 23 (2004) 5095–5098.
[23] D. Rubio, J. Garcia-Castro, M.C. Martin, R. de la Fuente, J.C. Cigudosa, A.C. Lloyd, A. Bernad, Spontaneous human adult stem cell transformation, Cancer Res. 65 (2005) 3035–3039.

TISSUE ENGINEERING
Volume 13, Number 2, 2007
© Mary Ann Liebert, Inc.
DOI: 10.1089/ten.2006.0185

A Reverse Transfection Technology to Genetically Engineer Adult Stem Cells

ARIMICHI OKAZAKI, M.Eng., JUN-ICHIRO JO, M.Eng., and YASUHIKO TABATA, Ph.D., D.Med.Sci., D.Pharm.

ABSTRACT

A new non-viral method of gene transfection was designed to enhance the level of gene expression for rat mesenchymal stem cells (MSCs). Pullulan was cationized using chemical introduction of spermine to prepare cationized pullulan of non-viral carrier (spermine-pullulan). The spermine-pullulan was complexed with a plasmid deoxyribonucleic acid (DNA) of luciferase and coated on the surface of culture substrate together with Pronectin of artificial cell adhesion protein. MSCs were cultured and transfected on the complex-coated substrate (reverse transfection), and the level and duration of gene expression were compared with those of MSCs transfected by culturing in the medium containing the plasmid DNA-spermine-pullulan complex (conventional method). The reverse transfection method enhanced and prolonged gene expression significantly more than did the conventional method. The reverse method permitted the transfection culture of MSCs in the presence of serum, in contrast to the conventional method, which gave cells a good culture condition to lower cytotoxicity. The reverse transfection was carried out for a non-woven fabric of polyethylene terephthalate (PET) coated with the complex and Pronectin using agitation and stirring culture methods. The two methods enhanced the level and duration of gene expression for MSCs significantly more than did the static method. It is possible that medium circulation improves the culture conditions of cells in terms of oxygen and nutrition supply and waste excretion, resulting in enhanced gene expression.

INTRODUCTION

THE RECENT ADVENT OF GENOME SCIENCES has elucidated genetic sequences that are related to disease occurrence and the proliferation and differentiation of cells for tissue repair. In addition, with the rapid development of cell biology and medicine regarding tissue regeneration, it has been possible to make use of various precursor and stem cells with high potential for proliferation and differentiation for cell therapy. However, because the cells are often not powerful therapeutically, it is of prime importance for successful cell therapy that a method of genetic cell engineering aiming at efficient activation and manipulation of cellular functions be developed. To achieve this genetic engineering of cells, virus carriers have mostly been used because of the high efficiency of gene transfection.[1–7] However, there are several problems to be resolved for clinical applications, such as the antigenicity and toxicity of the virus itself or the possibility of disease transfection. Therefore, efficient technology and methodology of gene transfection without virus vectors are expected.

Several research trials using non-viral gene carriers of cationized polymers and liposomes have been performed but do not always achieve the expected results in terms of transfection efficiency.[8–11] The level of gene expression is not as high as that of viral carriers, and the expression time period is generally short. As the conventional procedure of gene transfection, the non-viral carrier is complexed with a plasmid deoxyribonucleic acid (DNA) and then added to the cell culture medium for transfection. In this case, serum

Department of Biomaterials, Field of Tissue Engineering, Institute for Frontier Medical Sciences, Kyoto University, Kyoto, Japan.

cannot generally be added to the culture medium, although it is essential to maintain the correct biological conditions for cell culture. This is because the plasmid DNA carrier complex often interacts with serum components, leading to suppression of the ability of gene transfection.

In this study, a new transfection method is introduced to enable cell culture under better conditions in the presence of serum. Pullulan of polysaccharide was chemically cationized using spermine to prepare a non-viral carrier for gene transfection. It has been demonstrated that the cationized spermine-pullulan enhanced *in vitro* gene expression for various types of cells.[12] The spermine-pullulan complex of a plasmid DNA was coated onto a culture substrate together with a cell-adhesion substance, and then cells were cultured on the complex-coated substrate using different culture methods for gene transfection. The level and duration of gene expression using the new reverse transfection method were evaluated and compared with those of the conventional transfection method. We examine cytotoxicity after the reverse transfection.

MATERIALS AND METHODS

Materials

Pullulan with an average molecular weight of 47,300 was purchased from Hayashibara Biochemical Laboratories, Inc. (Okayama, Japan). Spermine was purchased from Sigma Chemical Co. (St. Louis, MO). Other chemicals were obtained from Nacalai Tesque. Inc. (Kyoto, Japan) and used without further purification.

Preparation of cationized pullulan derivative

Spermine was introduced to the hydroxyl groups of pullulan using an N,N′-carbonyldiimidazole (CDI) activation method.[13] Spermine (1.87×10^3 mg) and CDI (2.25×10^2 mg) were added to 50 mL of dehydrated dimethyl sulfoxide containing 50 mg of pullulan. Following agitation at 35°C for 20 h, the reaction mixture was dialyzed against ultra-pure double-distilled water (DDW) for 2 days with a dialysis membrane (cut-off molecular weight = 12,000–14,000, Viskase Companies, Inc, Willowbrook, IL). Then, the dialyzed solution was freeze-dried to obtain the spermine-introduced pullulan (spermine-pullulan). When determined from the conventional elemental analysis and expressed by the molar extent of spermine introduced to the hydroxyl groups of pullulan, the percentage of spermine introduced was 12.3 mole.

Preparation of plasmid DNA

The plasmid DNA used was the pGL3 vector (5.26 kb) coding for a firefly luciferase gene (Luciferase Reporter Vectors-pGL3, Promega, Madison, WI). The plasmid DNA was propagated in *E. coli* (strain DH5α) and purified using QIAGEN plasmid Mega kit (Qiagen K.K., Tokyo, Japan) according to the manufacturers' instructions. The yield and purity of the plasmid DNA were evaluated using ultraviolet spectroscopy (Ultrospec 2000, Pharmacia Biotech, Cambridge, England). The absorbance ratio at wavelengths of 260 to 280 nm for plasmid DNA solution was measured to be between 1.8 and 2.0.

Preparation of polyion complexes

Polyion complexes were prepared by mixing an aqueous solution of spermine-pullulan with that of plasmid DNA. Briefly, various amounts of spermine-pullulan were dissolved in 50 μL of DDW, mixed with 50 μL of phosphate-buffered saline solution (PBS, 10 mM, pH 7.4) containing 100 μL of plasmid DNA, and left for 15 min at room temperature to obtain various polyion complexes (PICs) of spermine-pullulan and plasmid DNA. The PIC composition was calculated on the basis of the nitrogen number of spermine-pullulan (N) per the phosphorus number of plasmid DNA (P) and expressed as the N/P ratio.

Preparation and culture of mesenchymal stem cells

Mesenchymal stem cells (MSCs) were isolated from the bone shaft of femurs of 3-wk-old male Wister rats according to the technique reported by Lennon *et al.*[14] Briefly, both ends of rat femurs were cut away from the epiphysis, and the bone marrow was flushed out using a syringe (21 gauge needle) with 1 mL of alpha minimum essential medium (αMEM) supplemented with 15 vol% fetal calf serum (FCS), penicillin (50 U/mL), and streptomycin (50 U/mL). The cell suspension (5 mL) was placed into two 25 cm^2 flasks (Iwaki Glass, Funabashi, Chiba, Japan) and cultured at 37°C in a 95% air, 5% carbon dioxide atmosphere. The medium was changed on day 4 of culture and every 3 days thereafter. When the cells of the first passage became sub-confluent, usually 7 to 10 days after seeding, the cells were detached from the flask using treatment for 5 min at 37°C with PBS solution containing 0.25 wt% trypsin and 0.02 wt% ethylenediaminetetraacetic acid. Cells were normally subcultured at a density of 2×10^4 cells/cm^2. Second-passage cells at sub-confluence were used for all experiments.

Conventional 2-dimensional transfection in the static method

Cells were seeded on each well of a 12 well multi-dish culture plate (Corning, NY) at a density of 5×10^4 cells/well and cultured in 1 mL of αMEM medium with 15 vol% FCS for 24 h. PICs were formed by mixing 50 μL of DDW containing spermine-pullulan and 50 μL of PBS containing 2.5 μg of pGL3-luciferase plasmid DNA at different N/P ratios. Immediately after the medium was exchanged using FCS-free αMEM medium, 100 μL of the PIC solution was added, and transfection culture was performed for 6 h (conventional transfection). After the medium was changed to

αMEM with FCS, cells were incubated further for 1, 3, 5, and 7 days.

Two-dimension reverse transfection in the static method

Succinic anhydride (90.1 mg) was added to 20 mL of 100 mg/mL gelatin solution in dimethyl sulfoxide, followed by agitation at room temperature for 18 h to allow the carboxyl groups to be introduced into the amino groups of gelatin for anionization. When determined as the extent of amino groups decreased using the tri-nitrobenzene sulfonic acid method,[15] the molar amount of carboxylic groups introduced was 100 mole%.

The aqueous solution of the anionized gelatin (100 μg/mL) and different amounts of Pronectin was placed into each well of a 12 well culture plate and left at 37°C for 1 h for coating. After PBS washing, the well was coated with the plasmid DNA-spermine-pullulan complex containing 2.5 μg of plasmid DNA. After 30 min incubation, the wells were washed with PBS. Then MSCs (5×10^4 cells/well) were seeded on the complex-coated well, followed by cell culture in the αMEM medium with or without 15 vol% FCS for 1, 3, 5, and 7 days.

Cells were washed with PBS once, lysed in 100 μL of cell culture lysis reagent (Promega Corp., Madison, WI), transferred into a micro reaction tube, and the cell debris separated using centrifugation (14,000 rpm, 20 min). Then 100 μL of luciferase assay reagent (Promega Corp., Madison, WI) was added to 20 μL of supernatant, and the relative light unit (RLU) of the sample was determined using a luminometer (MicroLumatPlus LB 96V, Berthold, Tokyo, Japan). The total protein of each well was determined using a bicinchonic acid (BCA) protein assay kit (Pierce, Rockford, IL) according to the manufacturers' instructions. The RLU was divided by the protein amount to normalize the influence of variance of number of cells on luciferase activity. Each experimental group was carried out 3 times independently.

Three-dimensional reverse transfection using different culture methods

Static, agitated, and stirring methods were used to culture MSCs in a non-woven fabric of polyethylene terephthalate (PET, fiber diameter 26 μm, 6 mm×3 mm) for their plasmid DNA transfection. A similar coating procedure with the complex and Pronectin was performed for the PET non-woven fabric. MSCs were seeded into the complex-coated 3-dimensional PET fabric using the agitation method reported previously.[16] Briefly, the non-woven fabric was placed in 0.5 mL of cell suspension (1×10^6 cells/mL), followed by agitation with an orbital shaker (Bellco Glass, Vineland, NJ) at 300 rpm for 6 h at 37°C. The cell-seeded non-woven fabric was thoroughly washed with the medium to exclude non-adherent cells. The MSC-attached PET fabric was incubated for 2, 5, and 8 days under the conventional static condition (static culture).

For the agitated culture method, the prepared MSC-attached PET fabric was placed in each well of a 6 well culture plate containing 6 mL of αMEM with 15 vol% FCS while the culture plate was agitated using the orbital shaker (Bellco Glass, Vineland, NJ) at 50 rpm for 2, 5, and 8 days. In addition, the MSC-attached fabric was fixed with a needle immobilized in the spinner flask, and 150 mL of medium was stirred at 50 rpm for 2, 5, and 8 days (stirring culture). To measure the level of gene expression for MSCs cultured using the static, agitated, and stirring methods, the PET fabrics were collected, and gene expression was assessed using a procedure similar to the one described above.

Cell viability

Cytotoxicity was assayed using a cell counting kit (Nacalai tesque, Inc., Kyoto, Japan). MSCs were transfected with 0.50 μg of free plasmid DNA or lipofectamine 2000 (0.50 μg) and the spermine-pullulan complexing 0.50 μg of plasmid DNA using the conventional and reverse methods for 2 days. Then the medium was changed to αMEM with FCS, and 100 μL of 2-(2-methoxy-4-nitrophenyl)-3-(4-nitrophenyl)-5-(2, 4-disulfophenyl)-2H- tetrazolium (WST-8) solution was added and the cells incubated for another 3 h. The absorbance of samples was measured at 450 nm using a VERSAmax microplate reader (Molecular Devices, Sunnyvale CA). The percentage cell viability was expressed as 100% for non-transfected, control cells.

Statistical analysis

Data were expressed as means ± standard deviations. Data were analyzed using 2-way analysis of variance, and then differences between means were analyzed using Fisher's protected least significant difference multiple comparison test, and significance was accepted at $p < 0.05$.

RESULTS

Gene expression for MSC using the conventional and reverse transfection methods

Table 1 and Fig. 1 show the level and duration period of gene expression after the reverse transfection of MSCs together with those of the conventional transfection. For the conventional method, in which the complex is added to the culture medium, the presence of serum suppressed the level of gene expression. Alternatively, a high expression level of MSCs transfected using the reverse method was observed even in the presence of serum. Moreover, the time period of gene expression was longer than with the conventional method. When reverse transfected in the absence of FCS, MSCs were detached from the culture substrate during the transfection culture (data not shown). Free plasmid DNA did not enhance gene expression, irrespective of the presence of serum. Fig. 2 shows the level of gene expression of MSCs

TABLE 1. LUCIFERASE EXPRESSION LEVEL OF MSC TRANSFECTED BY THE CONVENTIONAL AND REVERSE METHODS IN THE PRESENCE OR ABSENCE OF SERUM[a]

Transfection method		The level of gene expression (RLU/mg protein)	
		Free plasmid DNA	Plasmid DNA-spermine-pullulan complex
Conventional	FCS (−)	$(3.0 \pm 0.02) \times 10^3$	$(4.2 \pm 0.62) \times 10^6$
	FCS (+)	$(3.0 \pm 0.98) \times 10^3$	$(3.3 \pm 0.66) \times 10^5$
Reverse	FCS (−)	−	ND[b]
	FCS (+)	−	$(6.2 \pm 1.4) \times 10^7$

The level of gene expression for non-transfected, original MSC was 3.0×10^3 RLU/mg protein.

[a]The MSC were transfected in the static culture.

[b]The level could not be measured because of cell death.

Mean ± S.D.

using the reverse transfection method at different coating concentrations of Pronectin. Expression level was enhanced with greater coating concentration of Pronectin of adhesion substance.

Cell viability

Fig. 3 shows the cell viability of MSCs transfected using the conventional and reverse methods. Vell viability decreased significantly using the conventional transfection culture with the spermine-pullulan and Lipofectamine 2000

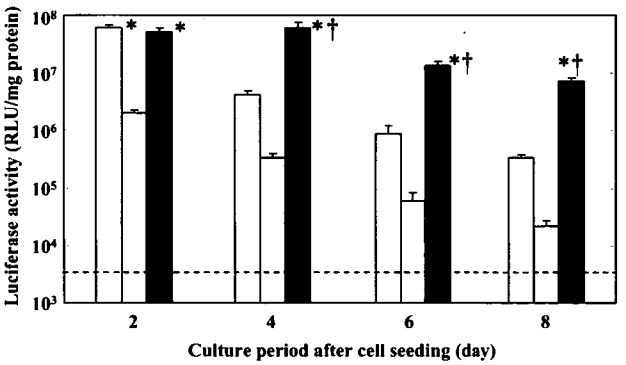

FIG. 1. Time course of luciferase expression level of mesenchymal stem cells (MSCs) transfected using the conventional (open and light gray columns) and reverse methods (solid columns) in static culture: (open columns) the plasmid DNA-spermine-pullulan complex in the absence of fetal calf serum (FCS) (dark gray columns), the plasmid DNA-spermine-pullulan complex in the presence of FCS, and (solid columns) the plasmid DNA-cationized pullulan complex in the presence of FCS. The dotted line indicates the level of non-transfected, original MSCs. $*p < 0.05$ versus the level in the presence of FCS using the conventional method at the corresponding time. $^{\dagger}p < 0.05$ versus the level in the absence of FCS using the conventional method at the corresponding time. RLU, relative light unit.

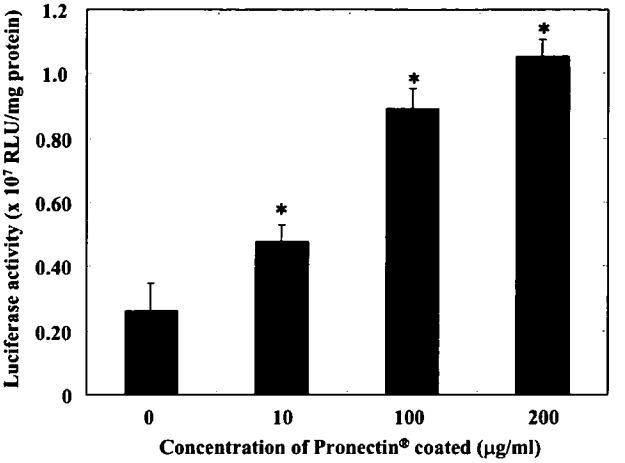

FIG. 2. Effect of Pronectin coating concentration on the luciferase expression level of mesenchymal stem cells (MSCs) transfected using the reverse method in the static culture. $*p < 0.05$ versus the luciferase activity of MSCs in the coating concentration of 0 μg/mL. RLU, relative light unit.

complexing plasmid DNA. On the contrary, the viability of cells after reverse transfection culture was similar to that of non-transfected, original cells.

Gene expression using 3-dimensional reverse transfection in different culture methods

Fig. 4 shows the time profile of gene expression of MSCs after reverse transfection using different culture methods.

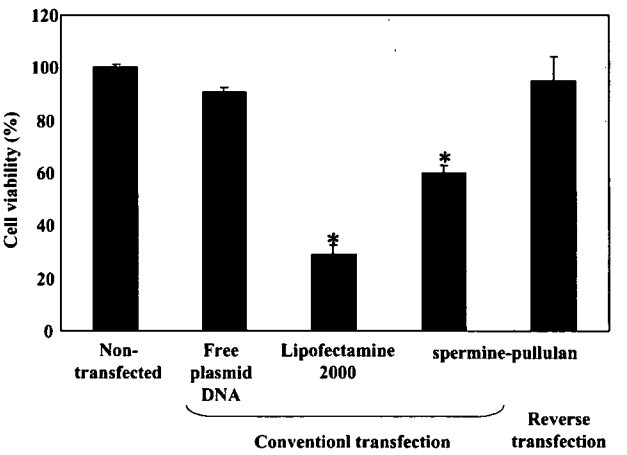

FIG. 3. Cell viability of mesenchymal stem cells (MSCs) 2 days after conventional and reverse transfection cultures. The cells were transfected using the conventional method with free plasmid deoxyribonucleic acid (DNA) or complexed with Lipofectamine 2000 and spermine-pullulan in the absence of serum. The cells were transfected using the reverse method with plasmid DNA-spermine-pullulan complex in the presence of serum. $*p < 0.05$ versus the cell viability of non-transfected, original MSCs.